minerals

MDPI

Article

Mineralogy and Geochemistry of High-Sulfur Coals from the M8 Coal Seam, Shihao Mine, Songzao Coalfield, Chongqing, Southwestern China

Qingfeng Lu [1,2,3], Shenjun Qin [2,*], Wenfeng Wang [1,3,4,*], Shihao Wu [2] and Fengjun Shao [3,4]

1 Jiangsu Key Laboratory of Coal-Based Greenhouse Gas Control and Utilization, Carbon Neutrality Institute, China University of Mining & Technology, Xuzhou 221008, China; luqingfeng@cumt.edu.cn
2 Key Laboratory for Resource Exploration Research of Hebei Province, Hebei University of Engineering, Handan 056038, China; wushihao8@163.com
3 Key Laboratory of Coalbed Methane Resources & Reservoir Formation Process, Ministry of Education, School of Resources and Geosciences, China University of Mining & Technology, Xuzhou 221008, China; sfj_leap@163.com
4 Institute of Geology and Mining Engineering, Xinjiang University, Urumqi 830002, China
* Correspondence: qinsj528@hebeu.edu.cn (S.Q.); wangwenfeng@cumt.edu.cn (W.W.)

Abstract: Mineral matter, including minerals and non-mineral elements, in coal is of great significance for geological evolution, high-value coal utilization, and environment protection. The minerals and elemental geochemistry of Late Permian coals from the M8 coal seam, Shihao mine, Songzao coalfield in Chongqing, were analyzed to evaluate the sediment source, sedimentary environment, hydrothermal fluids, and utilization prospects of critical metals. The average total sulfur (4.21%) was high in coals, which mainly exists in the forms of pyritic sulfur. Kaolinite, pyrite, calcite, quartz, illite and illite/smectite (I/S) mixed layers, and anatase predominated in coals, with trace amounts of chlorite, ankerite, and siderite. Epigenetic cell- and fracture-filling pyrite, veined calcite, and ankerite were related to hydrothermal fluids and/or pore water after the diagenesis stage. Compared to the world's hard coals, As and Cd are enriched in the Shihao M8 coals, and Li, Cr, Co, Zr, Mo, Pb, and Tb are slightly enriched. These high contents of sulfophile elements may be related to seawater intrusion. The terrigenous clastics of the Shihao M8 coals originated from the felsic–intermediate rocks atop the Emeishan Large Igneous Provinces (ELIP) (Kangdian Upland), while the roof and floor samples were derived from Emeishan high-Ti basalt. Through the combination of sulfur contents and indicator parameters of Fe_2O_3 + CaO + MgO/SiO_2 + Al_2O_3, Sr/Ba and Y/Ho, the depositional environment of peat swamp was found to be influenced by seawater. Although the critical elements in coal or coal ash did not reach the cut-off grade for beneficial recovery, the concentration of Li and Zr were high enough in coal ash.

Keywords: coal; geochemistry; minerals; associated elements; Southwestern China

Citation: Lu, Q.; Qin, S.; Wang, W.; Wu, S.; Shao, F. Mineralogy and Geochemistry of High-Sulfur Coals from the M8 Coal Seam, Shihao Mine, Songzao Coalfield, Chongqing, Southwestern China. *Minerals* **2024**, *14*, 95. https://doi.org/10.3390/min14010095

Academic Editor: Georgia Pe-Piper

Received: 27 November 2023
Revised: 10 January 2024
Accepted: 12 January 2024
Published: 15 January 2024

1. Introduction

Coal is the largest global distributed fossil resource, which dominates energy consumption in many coal-producing countries, especially in China, a scenario that is expected to continue for the foreseeable future [1]. Coal has properties of adsorption and reduction barriers [2], and it is composed of inorganic components (mineral matter) and organic matter or macerals [3]. The mineral matter primarily consists of non-mineral elements, crystalline minerals, and non-crystalline mineraloids [4]. As the essential components of coal, mineral matter is of great significance in coal geology, washing, combustion, gasification, liquefaction, and extraction [5–7]. The types, and modes of occurrence of minerals in coal are important factors affecting coal quality, and minerals are also the dominant carriers of associated elements in coal or coal ash [8].

Meanwhile, due to the trend of improving the energy consumption structure and environmental issues related to coal combustion, more attention has been paid to the comprehensively high-value exploitation of coal, as well as reducing environmental pollution [9–14]. Extensive geochemical studies on elements in coals have laid a good scientific foundation to realize the above purposes. On the one hand, critical elements including rare-metal (e.g., Li, Be, Nb, Ta, Zr, Sr, Hf, Rb, Cs), rare-scattered elements (e.g., Ga, Ge, In, Cd, Tl, Re, Se, Te), and rare-earth (REY, including 15 lanthanide elements plus Y, Sc) elements were found to be greatly enriched in coals and even formed coal-associate ores reaching the industrial cut-off grade [13,15–17], which makes coal deposits potential alternative raw sources of many deficient elements, particularly those of strategic importance. On the other hand, the high concentrations of hazardous elements, such as As, Cr, Co, Cu, Zn, Cd, Sb, Hg, Tl, Pb, etc., in coals and their releasing behaviors during combustion have been investigated widely, which has great practical benefits for environment protection [9,10,18].

The Late Permian coal in Southwestern China is one of the research topics of interest, attributed to its large reserve of 75 bt occupying 3% of the total coal reserves (depth of reserve calculation less than 1000 m) in China [10,19,20]. In this region, the enrichments of economically important elements including Nb, Ta, and Zr in the Zhina, Liuzhi, Huayingshan, Nantong, and Moxinpo Coalfields [16,21–24], and U, Mo, and V in the Guiding Coalfield [25], have been universally discovered. Moreover, other elements, such as Li, Cs, Ag, Re, etc., have also been sporadically reported in different coalfields. Meanwhile, the elevated environmentally sensitive elements, especially As, Se, Sb, Hg, Pb, Cr, V, Co, Cu, U, and Th, have been detected in the above and other coalfields in Southwestern China [9,10,26,27]. As was concluded from the available literature, relatively high concentrations of elements in Late Permian coals from Southwestern China are generally caused by various geological factors. The terrigenous material derived from Emeishan basalt should be the main provenance for these elements, and the influence of sea water or hydrothermal fluids, as well as volcanic activities, also contributes to the enrichment of certain elements [28,29]. However, the contents and occurrence modes of specific elements have been found to be diversified among Late Permian coals from adjacent or even the same coalfields in Southwestern China [22–24].

Mineral matter in coals can not only reflect geological information such as coal-forming depositional environment, coalification process, and geological historical evolution, but also provide relevant information on harmful elements such as As, F, Hg, etc. during coal combustion and utilization from the perspective of environmental protection. In addition, critical elements such as Ge, Ga, U, REY, etc. in coal and coal-bearing rocks can be enriched and mineralized under specific geological conditions, becoming useful associated mineral resources and improving the high-value utilization of coal. The Songzao coalfield, located in the southern part of Chongqing, hosts the abundant coal reserves in this region. Coals from the M8 coal seam, Shihao mine, Songzao coalfield, are characterized by low-volatile and high-sulfur anthracites. The high coal ranks (anthracites) characteristics of Shihao coals are inconsistent with much of the Late Permian middle–high-rank bituminous coals influenced by Emeishan basalt from Southwestern China. In order to provide comprehensive information regarding Late Permian coals in this region and help to achieve more systematically scientific perceptions, the samples from the M8 coal seam were selected for investigation in this study. In this study, the mineralogy and elemental geochemistry of the M8 samples were analyzed in detail to reveal the enrichment degree, sediment source, depositional environment, hydrothermal fluids, and evaluation of critical metals.

2. Geological Setting

The Shihao mine is located in Shihao town of Qijiang district, South Chongqing, and it is close to the junction of Chongqing and Guizhou provinces (Figure 1a–c). The Shihao mine is approximately 55 km and 115 km away from Qijiang district and Chongqing downtown, respectively. The coal mine is a rhombic shape on the plane, with a total area of about 22.3 km^2 (the N-S and E-W lengths are 7.2 km and 3.1 km, respectively). The Shihao

mine belongs to Songzao coalfield, one of the five coalfields of Chongqing (i.e., Songzao, Nantong, Zhongliangshan, Tianfu, and Yongrong coalfields) [27].

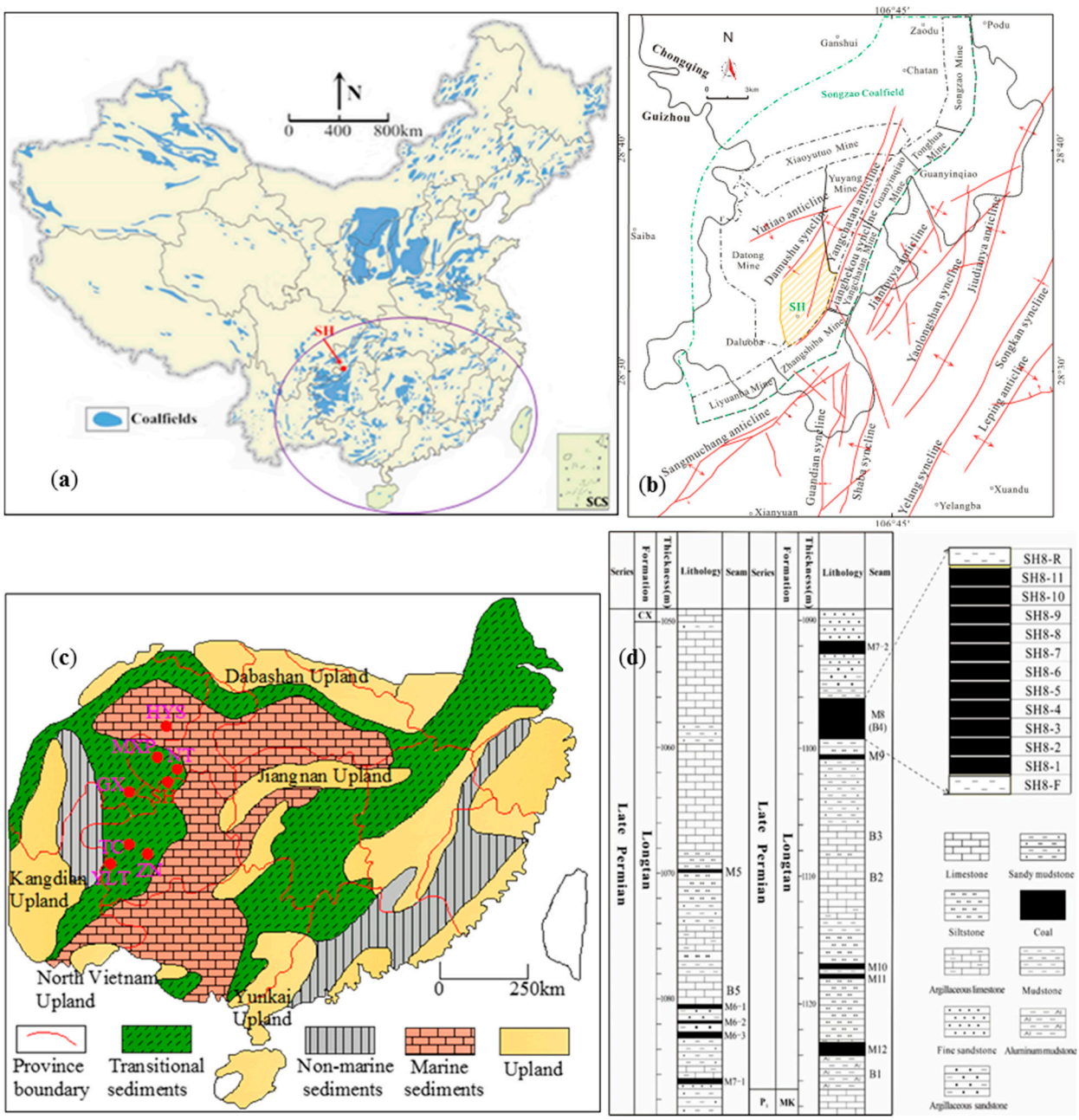

Figure 1. Location (**a**), tectonic (**b**), and paleography (**c**) of study area, and the stratigraphic column and samples numbers of the Shihao mine (**d**) (SH, Shihao; MXP, Moxinpo; HYS, Huayingshan; NT, Nantong; TC, Tucheng; ZN, Zhina; YLT, Yueliangtian; CX, Changxin Formation; MK, Maokou Formation; P_1, Early Permian).

The Shihao coal mine is located at the southwest of the 'bulge-type' tectonics, which formed by the third-order folds (Lianghekou and Damushu synclines, and Yangchatan and Yutiao anticlines) in the west of the Jiantouya anticline. The Jiantouya anticline is a secondary fold on the west of the Jiudianya anticline. The terrigenous supplies for coals in the Songzao coalfield were predominantly derived from the Kangdian Upland, which is an important sediment source region for coal basins from Chongqing, Western Guizhou, and Eastern Yunnan (Figure 1c) [30]. The exposed strata in this area range from Middle and Late Cambrian Loushanguan Formations ($Є_{2\text{-}3}ls$) to Late Jurassic Penglaizhen Formation (J_3p),

excluding Devonian and Carboniferous. The newest and oldest strata in the Shihao mine are Late Triassic Xujiahe Formation (T_3xj) and Early Permian Maokou Formation (P_1m), respectively. The dominated coal-bearing stratum in the Shihao mine is the Late Permian Longtan Formation (P_2l), which conformably underlies the Changxing Formation (P_2c) and unconformably underlies the Maokou Formation (P_1m) (Figure 1d) [30,31]. The coal-bearing sequence of P_2l in this area was developed and formed on the residual weathering crust caused by the Dongwu Movement, one of the essential tectonic events in Southwestern China [30]. The sedimentary environment of the P_2l is the tidal flat of restricted sea-carbonate platform of the continental-marine transitional environment [27]. The lithology of the P_2l primarily includes limestone, siltstone, mudstone, sandy mudstone, argillaceous limestone, fine sandstone, argillaceous sandstone, aluminum mudstone, and several coal seams (Figure 1d) [32]. Moreover, the fossils of plants and animals also exist within this stratum, i.e., gigantopteris, gigantonoclea, lepidodendron, and brachiopods. The thickness of coal-bearing strata (P_2l) ranges from 64.2 m to 82.3 m (av. 74.3 m), with eleven coal seams named M5 to M12 (Figure 1d). Coal seams can be divided into one full-area mineable seam (M8), three mostly area minable seams (M6-3, M7-2, and M12), and four locally minable coal seams (M5, M9, M10, and M11). According to the lithology and its distribution location of coal bearing strata in the Shihao mine, five marked layers are established (named B1 to B5, Figure 1d), i.e., aluminum mudstone, M8 coal seam, and three limestone layers. The M8 coal seam is located in the middle of the coal-bearing strata, with a thickness ranging from 1.5 m to 5.4 m (av. 3.2 m). The endogenous fractures are well developed in the M8 seam. The macroscopic characteristics of the M8 coal samples are semi-bright and semi-dull coals. The directly attached roof and floor rocks of the M8 coal seam are mudstone. The thickness of the other coal seams is generally less than 1 m. The M6-3 and M12 coal seams are mainly dark coal, followed by bright coal, which is semi-dark coal. Moreover, the M6-3 coal seam contains calcite veins and pyrite particles. The M7-2 coal seam is semi-bright coal, with relatively endogenous fissure and pyrite nodules. The direct roof and floor rocks of the M6-3 and M7-2 are argillaceous sandstone and fine sandstone, respectively (Figure 1d). The floor rock of M12 is gray and brown gray aluminum mudstone, with an average of 2.6 m, which is rich in pyrite nodules and locally existing siderite nodules.

3. Sample Collection and Analytical Methods

3.1. Sample Collection and Preparation

A total of 13 profile-samples were collected from the M8 coal seam in the underground working face of the Shihao mine following the Chinese standard of the coal and rock seam sampling method GB482–2008 [33]. The samples of the M8 coal seam were obtained over an area that was 10 cm wide, 10 cm deep, and 20 cm long. Firstly, the surface oxide layer of the coal seam was peeled off, and the surface of the coal seam was carefully leveled. Each layer of sample was marked on the surface of the coal seam up to a thickness of 20 cm. Meanwhile, the lithology, macroscopic characteristics, and other types of information were recorded in a book. A clean bag was laid at the bottom of the coal seam to pick up the fine samples. The layer samples were collected from the floor to roof of the M8 coal seam. The collected samples contained eleven coals (designated as SH8-1 to SH8-11 from the bottom to top), one roof (SH8-R), and one floor (SH8-F) (Figure 1d). Then, the samples were immediately sealed in clean plastic bags to prevent contamination and weathering. The samples were ground to pass 18-mesh (1 mm) and 200-mesh (0.075 mm) sieves for subsequent petrological and geochemical analyses, respectively.

3.2. Experimental Analytical Methods

The proximate analysis, including moisture, ash yield, volatile matter, and gross calorific value of the coals, was conducted following the Standards of ASTM D3173-11, D3174-11, D3175-11, and D5865-13, respectively [34–37]. In addition, the total sulfur and forms of sulfur were determined following the Standards of D3177-02 and D2492-02, respectively [38,39].

The mineralogical characteristics of the Shihao M8 coal were measured using a reflected light microscope (DM2500P, Leica, Wetzlar, Germany), X-ray powder diffraction (XRD, MAX2200PC, Rigaku, Tokyo, Japan), and field emission scanning electron microscopy–energy dispersive spectrum (SEM-EDS, SU8220, Hitachi, Tokyo, Japan). The polished grain mounts were prepared with the mixture of >18-mesh (<1 mm) raw coal with epoxy resin and curing agent according to the Chinese standard method GB/T 16773-2008 [40]. About 2 g raw coal particles were put into a mold with a diameter of 25 mm, and 6~8 g epoxy resin and curing agent (3:1) was added. Then, the mold was put into a Vacuum Mosaic machine (Poly' VAC) for solidification. After coarse and fine grinding (600-mesh, 1000-mesh, 2000-mesh, and 3000-mesh sandpapers) and polishing (alumina solution), the polished grain mounts were used to observe minerals via the Leica DM2500P microscope. The random reflectance of vitrinite (R_o) was measured using the Zeiss Axioskop 40 photometer system, with gadolinium gallium garnet (1.725%) as the standard material. Additionally, the morphology and elemental composition of minerals in the polished grain mounts were determined using SEM-EDS. In order to increase the electrical conductivity of polished grain mounts, gold was sprayed on its surface under the dry condition.

About 1 g 200 mesh coal was ashed in low-temperature oxygen plasma ashes (K1050X-D, Quorum, London, UK) to reduce or eliminate the effect of organic matter. The samples were reversed every 2 h to accelerate the ashing. This process ends when the sample quality does not change. Before testing, the ashed samples were flattened on a slide. Then, the minerals in the low-temperature ash (LTA) were determined using XRD with a step size of 0.02°. The quantitative analysis of minerals in LTA was conducted using Rietveld-based Siroquant^{TM} software V5 (Mitchell, ACT, Australia).

The major and trace elements in the samples were measured using an X-ray fluorescence spectrometer (XRF, ARL9800, Thermo Fisher Scientific, Waltham, MA, USA) and inductively coupled plasma mass spectrometer (ICP-MS, Thermal Elemental X-II, Thermo Fisher Scientific, Waltham, MA, USA), respectively. Particularly, As was determined using the atomic fluorescence spectrometer (AFS, XGY1011A, IGGE, Beijing, China). Specifically, 10 g 200 mesh samples were ashed at a high temperature (815 °C) in a muffle furnace with temperature programming. When the temperature of the maffle furnace dropped to room temperature, the samples were moved out and weighed. Then, boric acid and ash samples were added in the hydraulic channel and flattened using hydraulic press, where boric acid was at the bottom surface, such that the ash samples' surface had no cracks. Then, the flake samples were used for XRF testing. For trace-element detection, 40 mg of 200 mesh coal was digested by adding 1.5 mL of HNO_3, 0.5 mL of $HClO_4$, and 0.5 mL of HF into a PTFE bottle and reacted for 24 h at 150 °C. The digested solution was steamed until nearly dry on an electric heating plate, and then 1 mL of HNO_3 and 2 mL of H_2O (deionized water) were added to react for 3 h at 150 °C. Finally, the digested solution was diluted to 50 g using 2% HNO_3 for ICP-MS determination. The detection limit of V, Zn, Li, Ni, As, Rb, Th, Ba, Co, Cu, Ga, Sr, Mo, Cs, Sc, Tl, and Pb was greater than 0.2 μg/g; that of Be, Zr, Bi, Cd, Y, Nb, La, Ce, Pr, Nd, Sm, Gd, Yb, Hf, and In was greater than 0.005 μg/g; and that of Eu, Tb, Dy, Ho, Er, Tm, Lu, and U was greater than 0.003 μg/g.

4. Results

4.1. Coal Chemistry

The coal chemistry, including proximate analyses, sulfur, gross calorific, and vitrinite random reflectance of the Shihao M8 coals, is presented in Table 1. According to the average vitrinite random reflectance of 2.16%, the coals were generally classified as anthracites. The moisture, volatile matter (on a dry and ash-free basis), and ash (dry basis) were 1.71%, 15.4%, and 17.1%, respectively, indicating that the Shihao M8 coals are characterized by a low-moisture yield, volatile-matter yield, and low-medium ash yield. The coals exhibited high gross calorific values, with an average of 29.9 kJ/g. The total sulfur contents were at medium-high to high levels ranging from 1.73% to 7.45%, with an average of 4.21%.

The total sulfur contents were high in the upper and medium-lower parts of the M8 coal seam, such as SH8-1 to SH8-5 and SH8-10 to SH8-11. The dominant form of sulfur in the Shihao M8 coals was pyritic (3.18%), with trace amounts of sulfate and organic sulfur. The total sulfur contents of SH8-1, SH8-3 to SH8-5, and SH8-10 to SH8-11 were high because more pyrite existed in these coals, with the pyritic sulfur contents being 5.58%, 3.31%, 3.43%, 4.56%, 3.38%, and 5.29%, respectively. The inorganic sulfur (3.70%) was greater than the organic sulfur (0.52%), indicating the significant influence of seawater during the peat-forming process.

Table 1. The vitrinite random reflectance ($R_{o,ran}$), proximate and sulfur analyses (%), and gross calorific value ($kJ \cdot g^{-1}$) of M8 coals from Shihao mine.

Samples	$R_{o,ran}$	M_{ad}	A_{ad}	V_{ad}	A_d	V_{daf}	FC_d	$S_{t,d}$	$S_{p,d}$	$S_{s,d}$	$S_{o,d}$	$Q_{gr,d}$
SH8-11	2.19	2.25	15.5	13.8	15.9	16.7	70.0	7.12	5.29	1.18	0.65	30.1
SH8-10	2.02	1.51	12.4	12.7	12.6	14.8	74.5	4.69	3.38	0.42	0.89	32.2
SH8-9	2.08	1.25	15.6	11.1	15.8	13.4	73.0	2.73	2.40	0.12	0.21	31.2
SH8-8	1.95	1.16	10.8	10.9	10.9	12.3	78.2	2.21	1.79	0.03	0.39	33.2
SH8-7	2.10	1.24	11.6	10.9	11.7	12.5	77.3	2.27	2.06	0.10	0.11	33.0
SH8-6	1.95	1.17	10.5	10.8	10.6	12.2	78.4	1.73	1.13	0.02	0.58	33.2
SH8-5	1.86	2.35	16.5	14.6	16.9	18.1	68.1	5.92	4.56	0.87	0.48	29.2
SH8-4	1.90	1.59	18.2	13.2	18.5	16.4	68.2	5.81	3.43	0.69	1.70	29.5
SH8-3	2.00	1.84	19.5	13.3	19.8	16.8	66.7	4.10	3.31	0.61	0.18	29.5
SH8-2	2.09	1.81	16.9	11.7	17.3	14.4	70.9	2.33	2.07	0.10	0.15	29.9
SH8-1	2.20	2.70	36.8	13.1	37.8	21.6	48.7	7.45	5.58	1.53	0.34	18.1
Average	2.03	1.71	16.8	12.4	17.1	15.4	70.4	4.21	3.18	0.52	0.52	29.9

ad, air-dry basis; d, dry basis; daf, dry ash-free basis; R_o, random reflectance; M, moisture; A, ash yield; V, volatile matter; FC, fixed carbon; S_t, total sulfur; S_p, pyritic sulfur; S_s, sulfate sulfur; S_o, organic sulfur; Q_{gr}, gross calorific value.

4.2. Mineralogy

Minerals in coal samples are of great significance to a region's geological evolution and sedimentary environment [41]. Minerals contain important information originating in the syngenetic stage and can be altered during the epigenetic and diagenetic stages [42]. Meanwhile, minerals in coal also play an important role in coal utilization, which reduces the economic value of coal. Based on the observation and analyses of XRD, SEM-EDS, and reflected light microscope, the minerals in the Shihao M8 coals were obtained. Clay (kaolinite, illite and illite/smectite mixed layer, and chlorite), sulfide (pyrite), carbonate (calcite, ankerite, and siderite), oxides (quartz and anatase), and albite minerals predominate in coals, according to Table 2 and Figures 2–5. The roof and floor rocks of the M8 coal seam are mudstone, with high ash yields (87.76% and 91.75%), and they also contain large amounts of minerals. Minerals in the roof and floor primarily consist of kaolinite, pyrite, illite and illite/smectite mixed layer, quartz, and calcite. The content of bassanite in the floor rock is higher than that in the roof rock. The bassanite may be formed by the dehydration of gypsum ($CaSO_4 \cdot 2H_2O$), or it may be formed by the reaction of organic sulfur and organically bound calcium in coals during the low-temperature ashing process [43].

Table 2. The quantitative data of minerals in the Shihao M8 LTAs (%).

	Kao	Pyr	Cal	Qua	I/S	Alb	Ana	Rut	Sid	Bas	Chl
SH8-R	60.4	6.5	3.1	12.9	7.7	2.3	3.6	0.7	1.8	1	
SH8-11	50.4	37.8	2.7	2.2	2.3	2	1.1		1.5		
SH8-10	57.9	25.6	9.6	0.9	3	1.3	0.7		1		
SH8-9	68.8	14.6	7.9	1.2	1.8	1	4.2	0.5			
SH8-7	51.4	21.3	22.4	0.7	2	1.2	1				
SH8-5	25.6	22.6	4.7	0.4	38.4	3.1	0.2		1.3	1.7	2
SH8-3	66.2	17.4	5.7	3.1	5.1	2	0.5				

Table 2. *Cont.*

	Kao	Pyr	Cal	Qua	I/S	Alb	Ana	Rut	Sid	Bas	Chl
SH8-1	33.8	20.7	2.5	35.1	3.1	1.3	2.7	0.3			0.5
SH8-F	47.8	7.7	4.5	9.6	10.5	3.5	8.1	1.2		7.1	

Kao, Kaolinite; Pyr, pyrite; Cal, calcite; Qua, quartz; I/S, mixed-layer illite/smectite; Alb, albite; Ana, anatase; Rut, rutile; Sid, siderite; Bas, basanite; Chl, chlorite.

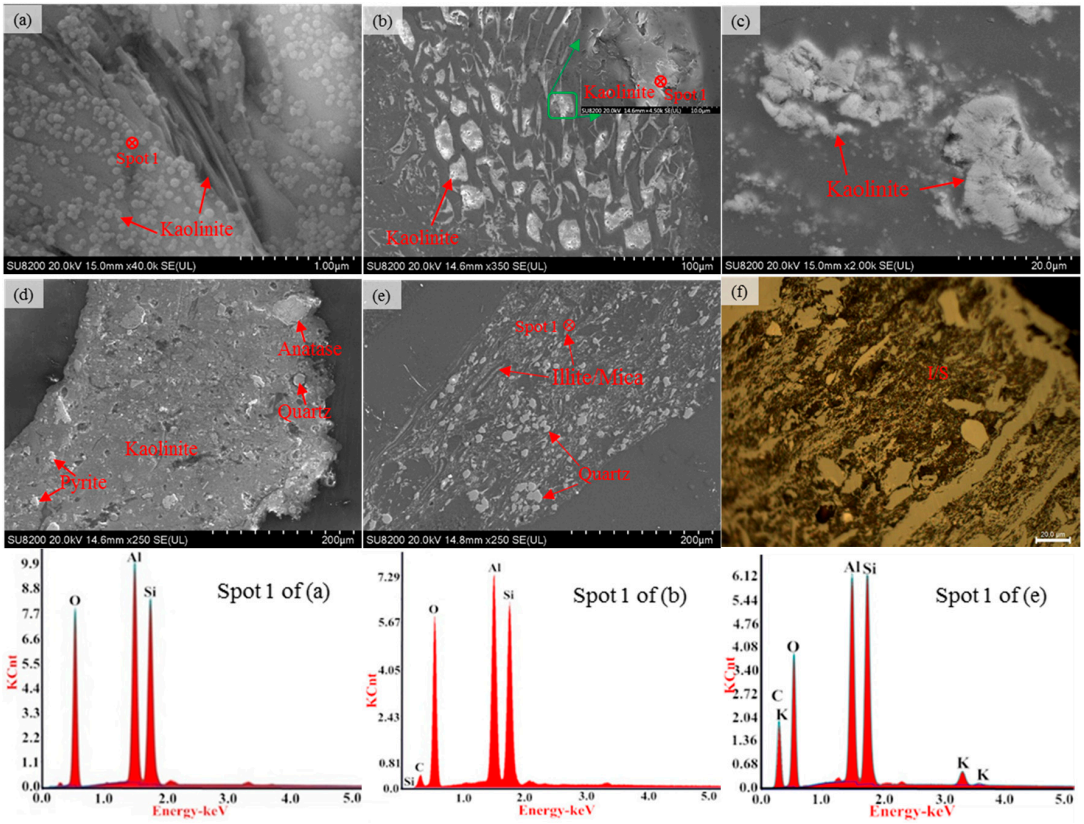

Figure 2. SEM-EDS images (**a**–**e**) and reflected light, immersion oil microphotographs (**f**) of the clay minerals in the Shihao M8 coals ((**a**,**c**) SH8-5; (**b**) SH8-9; (**d**–**f**) SH8-1).

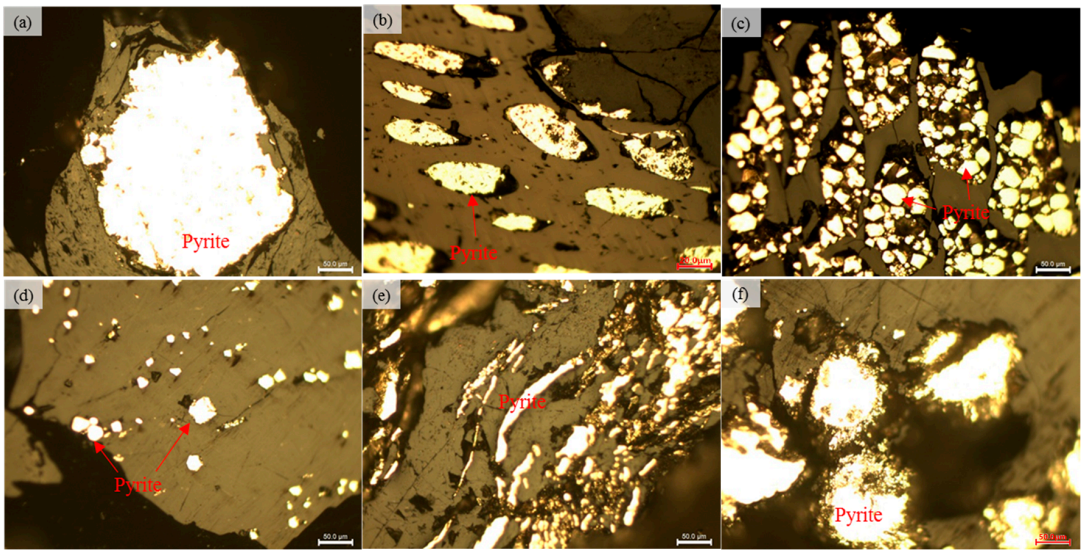

Figure 3. Reflected light, immersion oil microphotographs of sulfide minerals in the Shihao M8 coals ((**a**,**e**) SH8-3; (**b**) SH8-5; (**c**) SH8-9; (**d**,**f**) SH8-10).

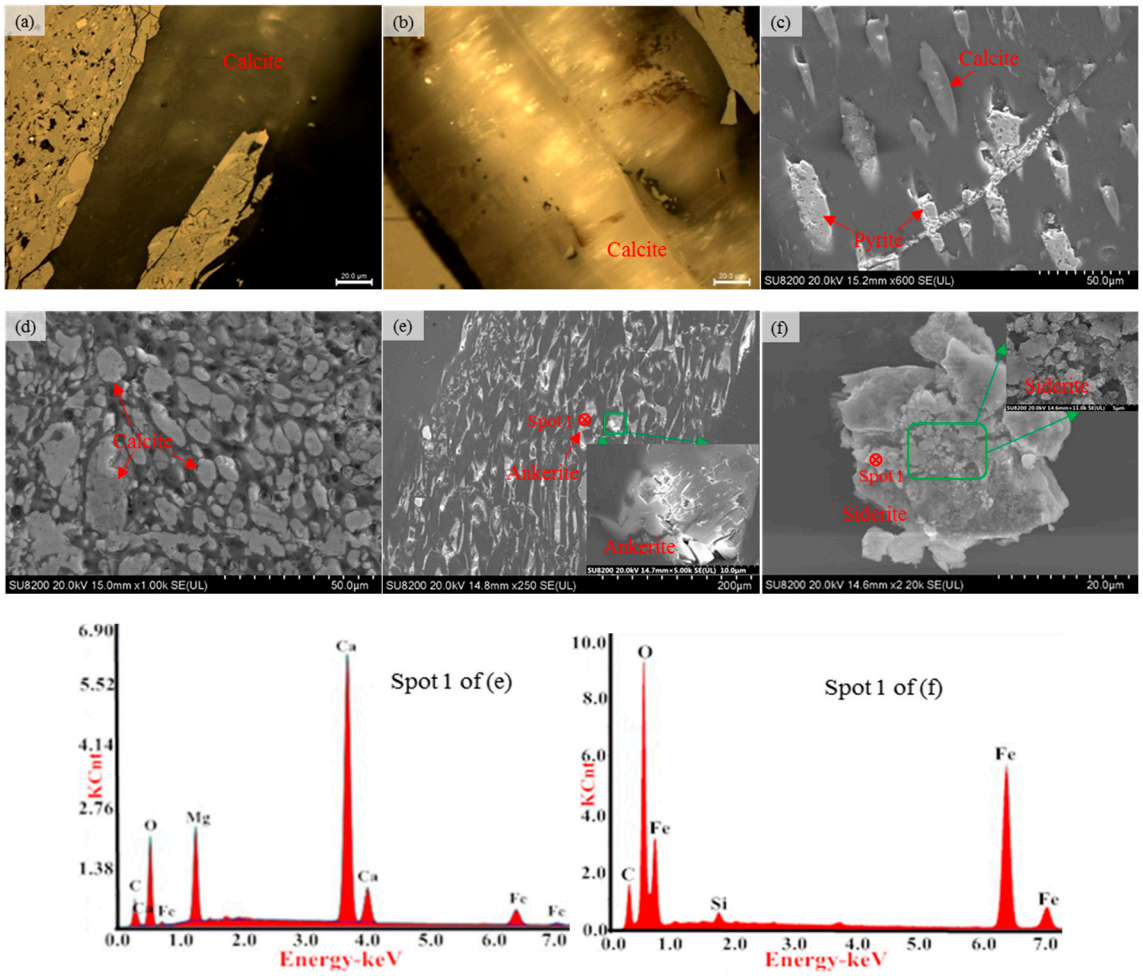

Figure 4. Reflected light, immersion oil microphotographs (**a**,**b**), and SEM-EDS images (**c**–**f**) of carbonate minerals in the Shihao M8 coals ((**a**,**e**,**f**) SH8-9; (**b**) SH8-10; (**c**,**d**) SH8-5).

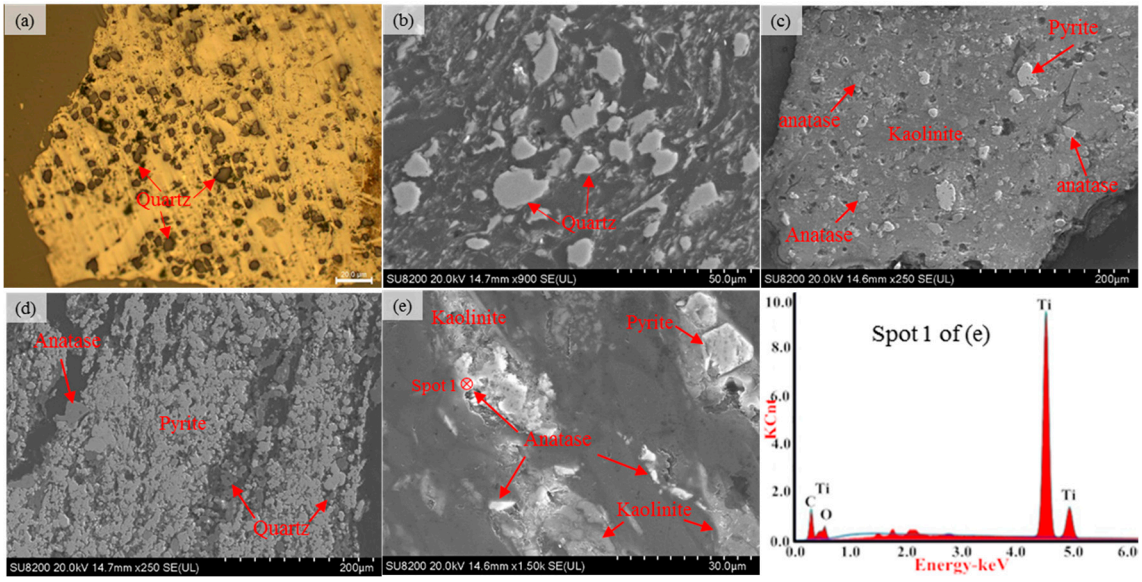

Figure 5. Reflected light, dry objective microphotographs (**a**), and SEM-EDS images (**b**–**e**) of oxide minerals in the Shihao M8 coals ((**a**–**d**) SH8-1; (**e**) SH8-9).

4.2.1. Clay Minerals

Clay minerals are essential minerals in coals and have an important influence on the occurrence and enrichment of associated elements [13]. Clay minerals in the Shihao M8 coals are dominated by kaolinite, followed by illite/smectite (I/S) mixed layer and illite, and lower amounts of chlorite (Table 2). Kaolinite in the Shihao M8 coals co-occurred with organic matter. The occurrence modes of kaolinite in coals primarily include discrete and zone fine particles (Figure 2a), cell-filling (Figure 2b), recrystallized vermicular textures (Figure 2c), and lumpy structures (Figure 2d). The cell-filling kaolinite has a lamellar structure under a high magnification (Figure 2b). Discrete and zonal kaolinite may indicate its derivation from syngenetic clastic sediments [27]. Cell-filling and wormy structured kaolinites are of epigenetic origin [44,45]. Cell-filling authigenic kaolinite may be formed by the reaction of silica-containing liquid with the void-filled hydroxides of aluminum at the early stages of peat accumulation and diagenesis [44]. Vermicular kaolinite is mostly distributed in tonsteins but also occurs in coals. The vermicular kaolinite predominantly comprises pseudomorphs after mica and feldspar [46]. Lumpy kaolinite in the Shihao M8 coals indicates terrigenous detrital origin [17]. Illite/Mica was detected in collodetrinite as long strips under SEM-EDS (Figure 2e). The I/S mixed clay layer occurs as a matrix in vitrinite (Figure 2f). Minerals, i.e., pyrite, quartz, chlorite, and anatase, commonly exist in the I/S mixed clay layer [45]. Chlorite, a rare mineral in coals, was detected in the XRD pattern analysis (Table 2).

4.2.2. Sulfide Minerals

Owing to the marine and terrestrial transitional environment of the Shihao coals, with high contents of total sulfur (pyritic sulfur), pyrite occurred in all the samples from the M8 coal seam, Shihao coal mine. Pyrite has five modes of occurrence in coals, including massive (Figure 3a), cell-filling (Figure 3b,c), subhedral to euhedral (Figure 3c,d), fracture-filling (Figure 3e), and framboidal (Figure 3f) structures. In particular, the subhedral to euhedral pyrite is not only dispersed in collotelinite (Figure 3d), but also filled in the cell cavity of the plant (Figure 4c). Cell-filling and fracture-filling pyrites in the Shihao M8 coals are of epigenetic origin [47]. Other morphological pyrites are of syngenetic origin. Due to its complete crystal shape, high euhedral degree, and small particle size, the framboidal and euhedral pyrite may be formed in the early syngenetic stage [48]. Massive pyrite was formed in the late syngenetic stage [31].

4.2.3. Carbonate Minerals

The carbonate minerals in the Shihao M8 coals primarily include calcite, ankerite, and siderite according to the XRD and SEM-EDS analyses. Ankerite and siderite were only detected in the SH8-9 and SH8-5 samples. There are three modes of occurrence of calcite in the Shihao M8 coals, including fracture-filling (Figure 4a,b), cell-filling (Figure 4c), and dispersed nearly rounded particles (Figure 4d). The fracture-filling calcite is filled in the organic components as a vein, indicating epigenetic origin. The twinning striation of the calcite can be seen under oil-immersed reflected light [49]. In particular, a certain proportion of calcite, with nearly rounded particles, also reflects an epigenetic origin. The occurrence modes of ankerite are similar to those of calcite, filling in the organic cavities or fracture (Figure 4e) [25]. A lower amount of lamellar and irregular siderite occurs in the collotelinite (Figure 4f), with a particle size of about 30 μm. Siderite is usually a typical syngenetic mineral in the peat formation stage, mostly formed in a weak oxidizing peat swamp environment [48].

4.2.4. Oxide Minerals

A certain proportion of quartz and anatase was observed in the Shihao M8 coals. Quartz in the Shihao M8 coal is mainly distributed as fine particles in a disseminated form associated with collodetrinite, with a size less than 30 μm (Figures 2e and 5a,b), indicating an authigenic origin. The titanium-containing oxides were detected through XRD analysis,

including anatase and a lower content of rutile. Meanwhile, titanium-containing oxides were also detected under the SEM-EDS. However, it is difficult to distinguish between anatase and rutile using SEM-EDS, because they have the same chemical composition. The quantitative analysis of minerals indicated a more general occurrence and high proportion of anatase than that of rutile in the studied coal samples. A very low proportion of rutile was detected in parts of the samples. Therefore, the titanium-containing oxides minerals detected under the SEM-EDS were identified as anatase in this study. Anatase occurred in the Shihao M8 coals as dispersed particles in the clay mineral matrix (Figure 5c); it was associated with pyrite in the collodetrinite (Figure 5d), filling the cell cavity of kaolinite (Figure 5e) with a particle size of approximately 5–30 μm. The dispersed anatase is a syngenetic mineral derived from the terrigenous clast (Figure 5c,d), while the cell-filling anatase is of epigenetic origin (Figure 5e).

4.3. Geochemistry

4.3.1. Major-Element Oxides and Trace Elements in Coal

The widely used concentration coefficient (CC, ratio of the researched sample content to the world's coals) for trace-element enrichment or depletion degree was proposed by Dai et al. [25]. The CC is divided into six levels, including depleted (CC < 0.5), normal (0.5 ≤ CC < 2), slightly enriched (2 ≤ CC < 5), enriched (5 ≤ CC < 10), significantly enriched (10 ≤ CC < 100), and anomalously enriched (CC ≥ 100). The contents of major-element oxides in the Shihao M8 coals are provided in Table 3. SiO_2, Al_2O_3, and Fe_2O_3 are the dominant major-element oxides in coals, accounting for 6.94%, 5.39%, and 3.10%, respectively, which can be confirmed by the major mineral matter of the Shihao coals (kaolinite and pyrite). The concentrations of other elements' oxides in coals display a descending trends in order of CaO, TiO_2, Na_2O, MgO, K_2O, P_2O_5, and MnO. The contents of major-element oxides are overall consistent with the sequence of that in Chinese coals [49]. The average concentrations of major-element oxides in the Shihao coals are lower than those in Chinese coals due to their low ash yield, except for TiO_2, with a concentration coefficient (CC) of 1.11 (Figure 6a). The content of TiO_2 in the coal samples is relatively higher, which is consistent with the result of anatase detected using XRD and SEM-EDS (Table 2, Figure 5). However, the relatively high CC ratios of some major elements, such as SiO_2, Al_2O_3, Fe_2O_3, and TiO_2, can be found among individual coal samples, especially in the SH8-1 sample taken near the floor. The content of TiO_2 in coal samples SH8-1 to SH8-4 and SH8-9 was slightly higher than that in Chinese coal, with a CC of 3.24, 1.15, 1.31, 1.18, and 1.25, respectively.

Table 3. Concentration of major-element oxides (%) in coals from the M8 coal seam, Shihao mine.

Samples	SiO_2	Al_2O_3	Fe_2O_3	CaO	TiO_2	K_2O	Na_2O	MgO	P_2O_5	MnO
SH8-R	39.9	27.0	6.52	0.63	3.63	1.95	1.80	0.741	0.252	0.031
SH8-11	4.49	4.01	6.20	0.27	0.23	0.036	0.084	0.065	0.011	0.003
SH8-10	3.87	3.76	3.63	0.47	0.16	0.032	0.084	0.058	0.010	0.003
SH8-9	6.53	5.97	1.74	0.45	0.41	0.073	0.080	0.084	0.012	0.003
SH8-8	4.39	4.13	1.29	0.28	0.30	0.048	0.061	0.058	0.036	0.002
SH8-7	4.66	4.49	1.37	0.36	0.28	0.040	0.061	0.060	0.053	0.002
SH8-6	4.93	4.40	0.51	0.17	0.23	0.058	0.056	0.060	0.008	0.001
SH8-5	5.10	5.09	4.79	0.74	0.13	0.063	0.063	0.087	0.013	0.005
SH8-4	6.88	6.61	3.04	0.66	0.39	0.059	0.073	0.082	0.015	0.004
SH8-3	7.87	7.22	2.81	0.53	0.43	0.075	0.073	0.084	0.014	0.002
SH8-2	7.95	5.91	1.94	0.33	0.38	0.057	0.064	0.068	0.011	0.002
SH8-1	19.6	7.65	6.84	0.49	1.07	0.235	0.186	0.160	0.022	0.004
SH8-F	43.2	30.4	2.37	0.33	4.59	3.667	1.820	0.835	0.085	0.006
SH-av.	6.94	5.39	3.10	0.43	0.37	0.071	0.081	0.079	0.019	0.003
Chinese	8.47	5.98	4.85	1.23	0.33	0.22	0.19	0.16	0.092	0.015

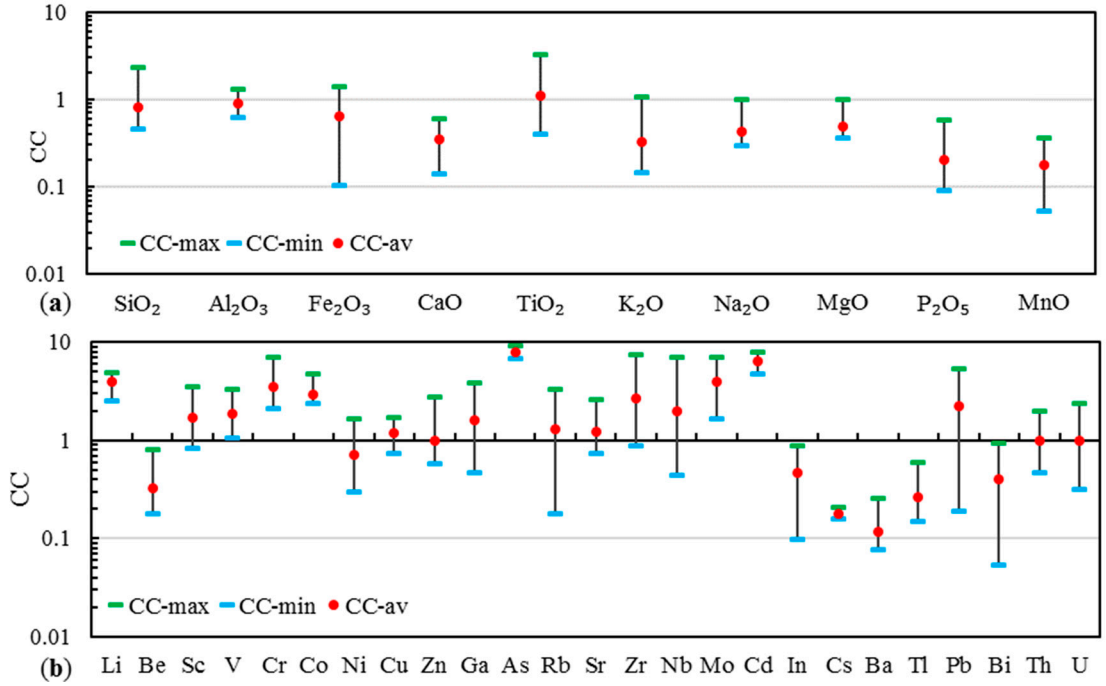

Figure 6. Concentration coefficients of major-element oxides (**a**) and trace elements (**b**) in the Shihao coal.

All major-element oxides are higher than that in the Shihao coals, except for Fe_2O_3 and CaO in the floor rock sample. SiO_2, Al_2O_3, Fe_2O_3, TiO_2, K_2O, and Na_2O are the primary components in the roof and floor rocks, with the proportions of 41.6%, 28.7%, 4.44%, 4.11%, 2.81%, and 1.81%, respectively. The concentration of SiO_2, Al_2O_3, TiO_2, K_2O, Na_2O, and MgO in the roof was slightly higher than that in the floor rock sample.

The contents of trace elements in the Shihao M8 coals are listed in Table 4. Compared to the world's hard coals, the coals were enriched in As and Cd, with a CC of 7.96 and 6.34, respectively (Figure 6b). Lithium, Cr, Co, Zr, Mo, and Pb were slightly enriched ($2 < CC < 5$). Be, In, Cs, Ba, Tl, and Bi in the Shihao M8 coals were significantly lower than that in the world's hard coals. Other trace-element contents in the Shihao M8 coals were close to the world's hard coals, with $0.5 < CC < 2$. Compared to the Upper Continental Crust (UCC), As, Mo, and Cd were significantly enriched; Li, Co, Cu, Nb, and Tb were enriched; Sc, V, Cr, Zn, Zr, Pb, La, Eu, Y, and Er were slightly enriched; Be, Rb, In, Cs, Ba, Tl, and Th were depleted; and other elements were normal in the roof and floor rock samples.

Table 4. Contents of trace elements in the Shihao M8 coals (μg/g).

Samples	Li	Be	Sc	V	Cr	Co	Ni	Cu	Zn	Ga	As	Rb	Sr	Zr	Nb	Mo	Cd	In	Cs	Ba
SH8-R	101	1.84	18.8	328	230	98.5	65.5	159	480	13.4	77.5	72.5	274	490	44.2	156	1.20	0.02	1.55	218
SH8-11	34.7	0.36	5.54	47.7	87.5	19.4	26.5	21.1	27.7	22.7	64.9	59.5	112	53.2	2.22	9.50	1.15	0.03	0.21	11.5
SH8-10	50.4	0.47	5.30	56.1	51.1	15.7	9.54	17.3	77.1	8.88	82.6	26.3	127	37.6	1.76	10.2	1.59	0.01	0.23	12.5
SH8-9	57.8	0.75	4.17	93.1	52.1	18.5	11.63	26.9	19.2	3.84	69.3	29.5	80.3	56.8	3.97	5.67	1.30	0.02	0.19	17.4
SH8-8	47.9	0.49	7.28	53.9	42.1	16.5	8.28	16.5	17.7	5.44	71.0	15.3	167	43.8	3.27	3.48	1.18	0.02	0.17	13.3
SH8-7	50.1	0.39	7.11	40.1	42.3	14.8	6.96	17.6	17.5	5.59	81.7	16.5	256	44.5	3.52	3.90	1.39	0.02	0.19	16.5
SH8-6	66.1	0.60	3.41	38.6	36.2	14.1	6.29	22.2	16.1	2.82	75.5	25.8	110	31.3	2.01	3.50	1.25	0.02	0.19	13.7
SH8-5	53.1	0.61	3.07	29.0	69.3	14.7	11.7	17.4	31.9	15.8	75.2	32.4	129	44.5	2.72	12.8	1.41	0.04	0.19	23.2
SH8-4	67.2	0.53	6.13	56.0	54.5	15.9	8.62	20.4	22.9	6.81	67.9	18.0	108	98.9	6.07	14.6	1.07	0.03	0.18	14.3
SH8-3	67.4	0.74	9.68	48.5	58.3	17.1	8.34	18.2	23.1	8.34	61.5	20.7	74.0	126	11.8	5.95	1.36	bdl	0.21	16.6
SH8-2	69.0	0.67	13.10	40.3	41.1	15.6	5.09	11.8	18.5	4.60	66.2	3.22	80.5	250	27.9	10.5	0.93	0.02	0.21	14.6
SH8-1	47.2	1.59	5.16	78.3	118	28.2	28.1	20.9	33.7	22.0	71.9	10.0	120	267	22.5	10.2	1.32	0.01	0.22	38.1
SH8-F	127	0.24	45.26	408	197	87.7	45.5	176	170	5.91	79.8	11.1	504	1324	152	67.6	1.66	0.01	1.55	323
SH-av.	55.5	0.65	6.36	52.9	59.3	17.3	11.9	19.1	27.71	9.71	71.6	23.4	124	95.8	7.97	8.21	1.27	0.02	0.20	17.4
World	14	2	3.7	28	17	6	17	16	28	6	9	18	100	36	4	2.1	0.2	0.04	1.1	150

Table 4. *Cont.*

Samples	Tl	Pb	Bi	Th	U	La	Ce	Pr	Nd	Sm	Eu	Gd	Tb	Dy	Y	Ho	Er	Tm	Yb	Lu
SH8-R	0.49	41.2	0.24	5.75	2.78	55.3	91.3	12.0	31.6	5.76	3.70	4.36	3.26	3.49	34.2	0.86	6.03	0.49	1.66	0.35
SH8-11	0.10	22.9	0.35	6.41	4.44	3.02	6.36	5.73	8.80	2.68	0.54	2.34	0.95	1.23	10.5	0.24	1.02	0.09	1.17	0.29
SH8-10	bdl	1.70	0.99	2.83	1.68	4.92	9.84	2.51	3.26	2.28	0.26	2.61	0.72	1.15	7.44	0.19	0.76	0.11	0.79	0.29
SH8-9	0.12	20.6	0.11	1.92	0.90	8.20	25.9	3.56	6.46	2.42	0.27	2.81	0.84	2.59	6.30	0.20	2.25	0.18	0.31	0.29
SH8-8	0.12	9.27	0.47	1.87	0.87	16.2	17.0	3.64	7.61	2.64	0.36	2.02	0.68	1.21	6.31	0.23	1.40	0.11	0.91	0.26
SH8-7	0.12	2.62	0.88	1.93	0.86	21.5	18.5	6.27	9.26	3.17	0.38	2.15	0.69	1.33	5.86	0.26	1.10	0.08	0.67	0.25
SH8-6	bdl	14.6	0.24	1.50	0.59	15.1	29.2	3.10	9.36	3.08	0.31	1.92	0.63	0.86	4.57	0.18	1.13	0.08	0.18	0.20
SH8-5	bdl	23.8	1.03	4.81	3.08	10.2	18.8	7.37	6.04	2.91	0.45	2.31	0.46	0.72	7.44	0.22	0.64	0.06	0.71	0.14
SH8-4	0.17	15.2	0.33	2.54	1.38	24.4	39.2	3.98	10.5	3.25	0.37	2.36	0.43	1.48	12.0	0.19	1.72	0.11	0.20	0.32
SH8-3	0.27	32.3	0.06	2.97	1.74	22.0	45.2	6.14	13.1	3.50	0.37	1.88	0.35	1.90	12.3	0.19	1.90	0.09	0.19	0.41
SH8-2	0.34	26.1	0.16	1.83	0.93	21.1	33.1	2.87	11.2	3.32	0.36	2.36	0.68	2.83	19.5	0.17	1.94	0.09	0.30	0.33
SH8-1	0.17	48.6	0.22	6.26	4.34	26.9	45.8	5.19	14.0	4.03	0.56	3.57	0.75	2.15	31.8	0.24	3.71	0.17	0.38	0.29
SH8-F	0.11	67.0	0.25	1.09	0.94	88.1	150	12.6	69.7	6.82	3.92	6.09	3.50	3.22	62.4	1.35	8.69	0.79	1.87	0.72
SH-av.	0.15	19.8	0.44	3.17	1.89	15.8	26.3	4.58	9.06	3.03	0.38	2.39	0.65	1.59	11.3	0.21	1.60	0.11	0.53	0.28
World	0.58	9	1.1	3.2	1.9	11	23	3.4	12	2.2	0.43	2.7	0.31	2.1	8.2	0.57	1	0.3	1	0.2

4.3.2. Rare Earth Elements and Yttrium

The ratio of Ba to Eu in the sedimentary rocks or coals was used to judge the interference of Ba on Eu [50]. If the Ba/Eu is greater than 1000, Ba will interfere with the concentration of Eu. The values of Ba/Eu in the Shihao M8 coals were lower than 1000, ranging from 21.25 to 82.56, indicating that Ba has no interference on Eu concentration (Figure 7a). The total REY concentration in the Shihao M8 coals varied from 37.1 μg/g to 139 μg/g (on average 77.7 μg/g), which is slightly higher than that in the world's hard coals (68.41 μg/g) [51]. The REY in the Shihao M8 coals was dominated by LREY (58.7 μg/g), followed by MREY and HREY, with 16.3 μg/g and 2.72 μg/g, respectively (Figure 7b). Compared to the world's hard coals, the concentration coefficient of Tb was slightly enriched (CC = 2.10), while Ho and Tm were depleted (CC < 0.5) in the Shihao M8 coals (Figure 7c). The average concentrations of La, Ce, Pr, Sm, Y, Er, and Lu were slightly higher than those in world hard coals, with CC higher than 1. The concentrations of Nd, Eu, Gd, Dy, and Yb were lower than that in the world's hard coals. However, the concentrations of the roof and floor rock samples were 419 μg/g and 254 μg/g, which were higher than that of Upper Continental Crust (UCC, 168.37 μg/g) [52].

The geochemical parameters of REY were calculated in Table 5. The distribution patterns of REY are depicted in Figure 7d–f, which are normalized to UCC. The values of LREY/HREY and LREY/MREY in the Shihao M8 coals were 22.2 and 4.00, respectively, indicating that REY has a significant fractionation. Owing to the lower values of $(La/Lu)_N$ (<1), the REY enrichment patterns of the Shihao M8 coals were H-type. The average values of δEu and δCe were 0.56 and 0.70, respectively, indicating the negative anomalies for Eu and Ce in the Shihao M8 coals. The REY enrichment patterns of the roof and floor were L-type, with an La/Lu normalization of 1.66 and 1.31, respectively. The δEu and δCe of the roof and floor samples were positive and weak negative anomalies, with average values of 1.62 and 0.90, respectively.

Table 5. Geochemical parameters of rare earth elements and yttrium in the Shihao M8 coals.

Sample	L/M	L/H	M/H	$(La/Lu)_N$	$(La/Sm)_N$	$(Gd/Lu)_N$	Type	δEu	δCe
SH8-R	3.99	20.9	5.22	1.66	1.44	1.04	L	1.66	0.81
SH8-11	1.71	9.45	5.53	0.11	0.17	0.67	H	0.69	0.22
SH8-10	1.87	10.7	5.72	0.18	0.32	0.77	H	0.41	0.59
SH8-9	3.63	14.4	3.95	0.31	0.51	0.83	H	0.39	1.04
SH8-8	4.45	16.2	3.63	0.66	0.92	0.65	H	0.55	0.51
SH8-7	5.64	24.8	4.40	0.92	1.02	0.73	H	0.52	0.36
SH8-6	7.21	33.7	4.67	0.82	0.74	0.83	H	0.46	0.97
SH8-5	3.98	25.6	6.44	0.77	0.52	1.38	H	0.77	0.43
SH8-4	4.88	32.0	6.54	0.82	1.13	0.62	H	0.60	0.89

Table 5. *Cont.*

Sample	L/M	L/H	M/H	$(La/Lu)_N$	$(La/Sm)_N$	$(Gd/Lu)_N$	Type	δEu	δCe
SH8-3	5.35	32.3	6.04	0.57	0.94	0.39	H	0.60	0.88
SH8-2	2.78	25.3	9.09	0.68	0.95	0.60	H	0.49	0.94
SH8-1	2.47	20.0	8.10	1.01	0.99	1.05	L-M	0.64	0.88
SH8-F	4.13	24.4	5.90	1.31	1.94	0.72	L	1.58	0.99
Average	4.00	22.2	5.83	0.62	0.75	0.77		0.56	0.70

N, REY in coals normalized to upper continental crust (UCC); $\delta Ce = Ce_N/Ce_N^* = Ce_N/(0.5 \times La_N + 0.5 \times Pr_N)$; $\delta Eu = Eu_N/Eu_N^* = Eu_N/(0.67 \times Sm_N + 0.33 \times Tb_N)$; $\delta Y = Y_N/Ho_N$.

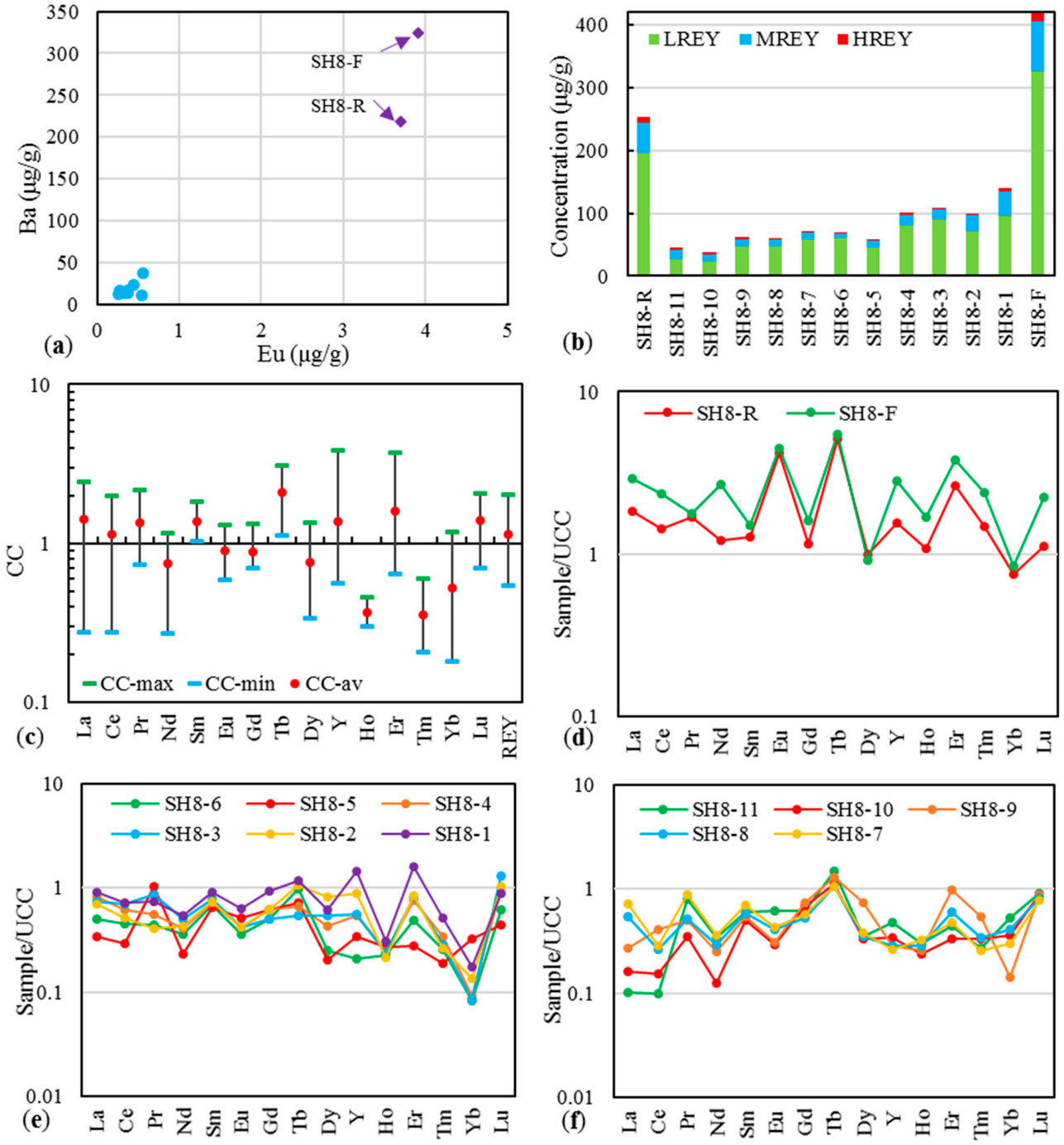

Figure 7. Relationship between Ba and Eu (**a**); concentrations of LREY, MREY, and HREY (**b**); CC of individual REY (**c**); UCC-normalized REY distribution patterns (**d**–**f**) of the Shihao M8 samples.

5. Discussion

5.1. Sediment Sources

The ratio of Al_2O_3 to TiO_2 is an effective provenance indicator for sedimentary rocks and for the sediment source region of coal deposits [53]. Specifically, the ratios among 3–8, 8–21, and 21–70 indicate that the sediments originate from mafic, intermediate, and felsic igneous rocks, respectively [42]. The Al_2O_3/TiO_2 ratios of the coal samples ranged from 7.14 to 38.2 (on average 18, Figure 8a,b), indicating that the original terrigenous clastics providing most inorganic elements in the Shihao M8 coal mainly derive from the weathered and oxidized felsic-intermediate rocks from the Emeishan basalt atop the Kangdian Upland [42]. In particular, the coal sample of SH8-1 had a high proportion of TiO_2 (1.07%), with a low Al_2O_3/TiO_2 value, which may be influenced by the immediate attached floor sample. This result was inferred from the high TiO_2 content (4.59%) in the floor rock and the presence of Ti-containing oxides in SH8-1 (Figure 5c,d) detected via SEM-EDS. The redox-sensitive elements Eu and Ce may be anomalous in coals and associated host rocks in certain circumstance [54]. Eu commonly displays negative anomalies in coals with the input of felsic–intermediate or felsic terrigenous debris, but positive anomalies in coals with mafic rocks or those affected by high-temperature hydrothermal fluids [55]. The felsic and felsic–intermediate igneous rocks are characterized by negative Ce anomalies [56], and coals derived from these rocks have weak Ce anomalies [55]. Eu and Ce exhibited negative anomalies ($\delta Eu < 1$, $\delta Ce < 1$), inferring that felsic or felsic–intermediate igneous rocks are the predominant terrigenous materials in the Shihao coals. Additionally, some typical Late Permian coals from Southwestern China were selected for comparison with the Shihao M8 coals, including Moxinpo K2 (MXP-K2) and Songzao No.8 (SZ-8) coals from Chongqing, Tucheng No.3 (TC-3) and Yueliangtian No.10 (YLT-10) coals from Guizhou, and Guxu No.25 (GX-25) coal from Sichuan. The provenance area Kangdian Upland supplied the most materials for the accumulation of sediments and inorganic matter of the peat, and it determined the elemental concentration in the Late Permian coals [57]. The relationship between Al_2O_3 and TiO_2 of Late Permian coals is illustrated in Figure 8c, with the values of Al_2O_3/TiO_2 higher than 8, indicating felsic or felsic–intermediate igneous input. Meanwhile, the elements of Eu and Ce in these coals also displayed negative anomalies, which is consistent with the Shihao M8 coals.

Rare earth element and yttrium have similar geochemistry properties and behaviors, and they mainly exist in the +3 valence state, i.e., Ce^{3+}, Eu^{3+}, Y^{3+}. As one of redox-sensitive elements, Eu^{3+} can be reduced to Eu^{2+} in reducing conditions and high temperatures [55]. The anomaly value of Eu (0.56) in the Shihao M8 coal indicates a strong negative anomaly, which is probably affected by the reducing and high-temperature environment. The Late Permian SH-M8, SZ-8, and GX-25 coals were classified as anthracites; however, other coals of TC-3 and YLT-10 coals and MXP-K2 coal were classified as medium- and high-rank bituminous coals, respectively. The high degree of coalification of the coal samples from the Songzao and Guxu coalfields is inferred to be related to the accumulation of mantle source materials from the Emeishan mantle plume [58]. The areas of Southwest Chongqing and South Sichuan belong to the accumulation range of mantle source materials, and they are subject to the thermal energy conduction of deep high-temperature mantle source materials. These two areas store thermal energy and become high-temperature anomaly areas, which is the main factor for the formation of Late Permian high-rank coals (anthracite).

The ratios of Al_2O_3 to TiO_2 in the roof and floor rock samples were low, with values of 7.46 and 6.62 (Figure 8a), indicating that the sediment sources of the rock samples were dominated by mafic rocks. The relationship between Al_2O_3 and TiO_2 of high-Ti basalt and low-Ti basalt is illustrated in Figure 8c. The Al_2O_3/TiO_2 values of the roof and floor in the Shihao mine are consistent with the high-Ti basalt. Meanwhile, the roof and floor samples represented positive Eu anomalies, and they had high concentrations of TiO_2, K_2O, and Sc, which is consistent with the high-Ti basalt from the Emeishan Large Igneous Province (ELIP) of the Kangdian Upland [59] (Figure 8d). Moreover, the high contents of anatase in the rock samples were identified via XRD testing (Table 2).

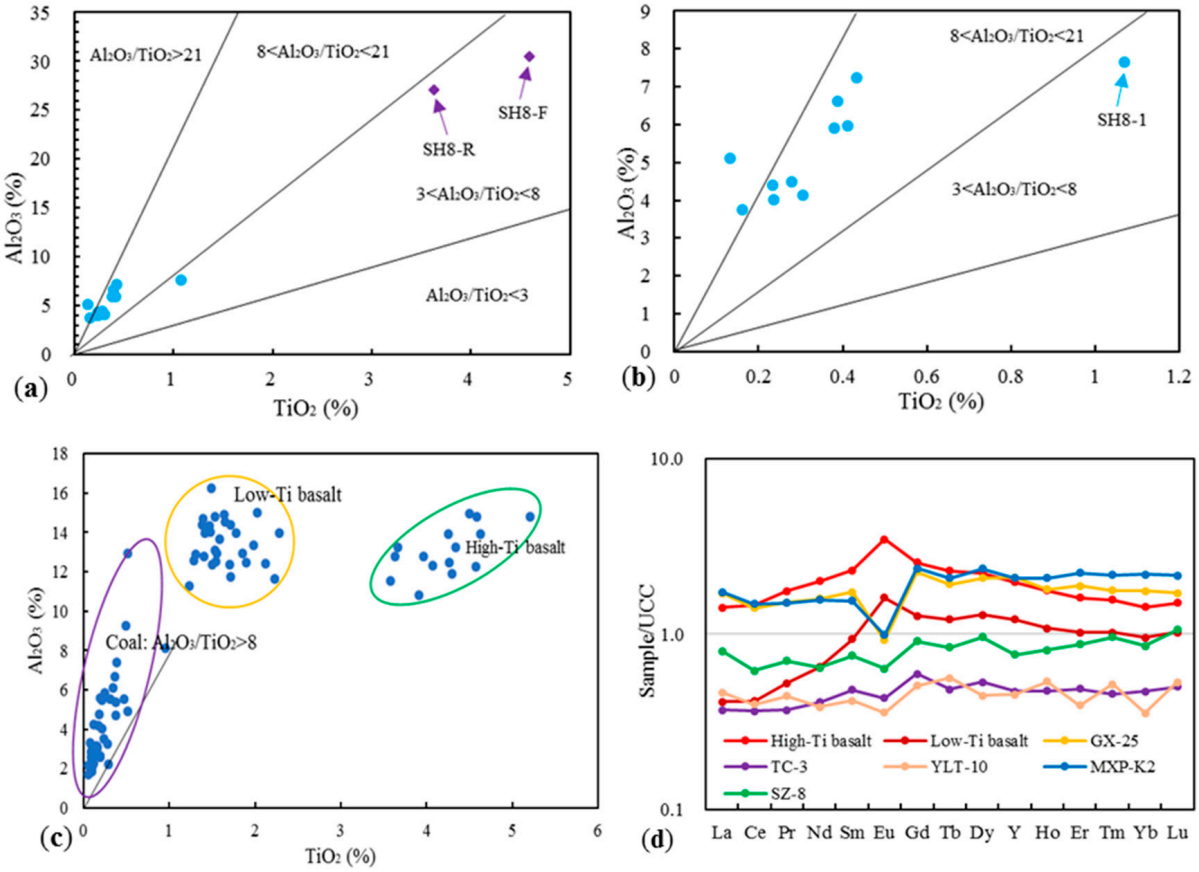

Figure 8. Relationship between Al_2O_3 and TiO_2 of all samples (**a**) and coals (**b**) in the Shihao coal (purple points are roof and floor rock samples), and the relationship of TiO_2 vs. Al_2O_3 and REY distribution patterns of high-Ti basalt, low-Ti basalt, and some Late Permian coals from Southwestern China (**c**,**d**); GX-25, Guxu, Sichuan; TC-3, YLT-10, Tucheng and Yueliangtian, Liupanshui, Guizhou; MXP-K2, Moxinpo, Chongqing; SZ, Songzao, Chongqing.

5.2. Depositional Environment

The Shihao M8 coals displayed high total sulfur contents, with an average of 4.21% and the highest value of 7.45%, dominated by pyritic sulfur (accounting for 78% of the total sulfur). These high-sulfur contents reflect a seawater-influenced environment of the coal seam [60]. When the coal-bearing basin is invaded by seawater, the Ca^{2+} and Mg^{2+} in the seawater will be precipitated under weak alkaline conditions, and Fe will be converted into Fe-containing minerals (i.e., pyrite) in a relatively reduced environment, which increases the contents of Fe, Ca, and Mg in the coal ash. When the influence of seawater is small, the coal ash composition mainly comes from the supply of terrigenous detrital (mainly the weathered basalt with high Si and Al) [61,62]. Therefore, the coal ash component index (AI) of $(Fe_2O_3 + CaO + MgO)/(SiO_2 + Al_2O_3)$ is a typical parameter that indicates terrestrial (AI < 0.23) and marine-influenced (AI > 0.23) peat swamps [62]. The parameter AI ranging from 0.08 to 0.77 (on average 0.31) verifies that the Shihao M8 coal was deposited under the marine-influenced reductive environment, i.e., in a tidal flat along the margin of the epicontinental sea basin. Meanwhile, Sr has a relatively high concentration in marine sediments, leading to a high value of Sr/Ba. The Sr/Ba was successfully used as an indicator for the marine-influence peat sedimentary environment [63]. Values of Sr/Ba that are greater and less than 1 reflect the marine- and fresh water- influenced coals, respectively [63]. The average ratio of Sr/Ba in the Shihao M8 coals was 7.89, indicating that the peat depositional environment was influenced by seawater intrusion. Seawater also has a significant influence on the concentration of Y in sediments. The values of Y/Ho

varied from 60 to 70 and 25 to 30, demonstrating that the sediments were affected by seawater and siliciclastic materials [29]. The ratios of Y/Ho in the Shihao M8 coals ranged from 22.5 to 130 (on average 54.0), revealing that the peat swamp suffered the distinct seawater intrusion.

5.3. Hydrothermal Fluid Injections

Hydrothermal fluid plays an important role in mineral and associated elements in Southwestern China coals. It also has an influence on the mineralogical properties of the Shihao coals. Cell-filling and fracture-filling pyrites in the Shihao M8 coals reflect the solution deposition during different coal-forming stages (Figure 3b,c,e) [64]. Cell-filling veined calcite may be the precipitated product of a Ca^{2+}-rich solution in the cell cavities during the syngenetic and/or early diagenetic stages [65]. Quartz in the Late Permian coals was primarily derived from the large amount of SiO_2 re-leased from the weathering and denudation of the Emeishan basalt atop the Kangdian Upland [66]. The released SiO_2 was injected into the peat swamp with the water flow, and it precipitated under special geological conditions. Then, it evolved into quartz in the subsequent diagenetic processes [62]. Ilmenite is probably formed by iron entering the lattice of anatase under the hydrothermal fluid activity [67]. Ankerite is mainly formed by the precipitation of the pore solution rich in Ca^{2+}, Mg^{2+}, and Fe^{2+} [68], suggesting pore-water deposition during the syngenetic and/or early diagenetic stages.

5.4. Evaluation of Critical Metals

In this study, critical metals, i.e., Li, Sc, V, Ga, Nb, Zr, and REY, were selected to evaluate the potential economic values in coals from the full-area mineable seam (M8) of the Shihao coals. Some essential contents of selected critical metals in the world's or Chinese coals or ash are listed in Table 6. Meanwhile, the corresponding concentrations of these elements in the Shihao M8 coal were also calculated.

Table 6. Concentrations of selected critical elements (μg/g).

Elements	World's Hard		Chinese Coal	Cut-off Grade		Shihao		
	Coal	Coal Ash		Coal Basis	Ash Basis	Coal	Coal Ash	CC-Coal Ash
Li	14.0	82.0	31.8/28.9	120	-	55.5	371	4.52
Sc	3.70	24.0	4.38	-	100	6.40	41.8	1.74
V	28.0	170	35.0	-	1000	52.9	341	2.01
Ga	6.00	36.0	6.55	30	100	9.70	57.4	1.59
Nb	4.00	22.0	9.44	-	300	7.97	42.7	1.94
Zr	36.0	230	89.5	-	2000	95.8	524	2.28
REY	68.4	445	136	300	1000	77.7	566	1.27

Lithium and Zr were slightly enriched in the Shihao M8 coals, with a CC of 3.97 and 2.66, respectively. The concentrations of Nb, V, Sc, Ga, and REY were normal, with values of 1.99, 1.89, 1.72, 1.62, and 1.14. However, the average concentration of Li in the Shihao coals was lower than its cut-off grade (120 μg/g). Similarly, Sc, V, Ga, Nb, and Zr in the Shihao coal ashes were lower than their corresponding cut-off grades on an ash basis. Owing to the low ash yield of the coals, the concentrations of Li, Zr, and V in the Shihao coal ashes were 4.52, 2.28, and 2.01 times (slightly enriched) higher than that in the world's coal ash. There are two criterions to assess the REY prospect, including the grade of REY oxides and the outlook coefficient (C_{outl}) [69]. Although the C_{outl} of the Shihao coals had a promising utilization prospect (on average 0.87), the average concentration of REY oxides (ranging from 344 μg/g to 782 μg/g) was lower than the cut-off grade of 1000 μg/g. Therefore, REY in the Shihao coals has no economic utilization value.

6. Conclusions

The Shihao M8 coals were generally characterized by low moisture and volatile matter yields, low-medium ash yields, and medium-high to high sulfur. The total sulfur contents were high in the upper and medium-lower parts of the M8 coal seam. The forms of sulfur were predominantly pyritic, with trace amounts of sulfate and organic sulfur. The minerals in the Shihao M8 coals were primarily composed of clay (kaolinite, illite and I/S mixed layer, and chlorite), sulfide (pyrite), carbonate (calcite, ankerite, and siderite), oxide (quartz, anatase), minerals, albite, and bassanite. Cell-filling or fracture-filling kaolinites, pyrites, and calcites in the Shihao M8 coals are of epigenetic origin. Lumpy kaolinites are derived from terrigenous detrital inputs. Massive, framboidal, and subhedral to euhedral pyrites are of syngenetic origin. Quartz in the Shihao M8 coals is of authigenic origin. The minerals in the roof and floor samples were mainly kaolinite, quartz, pyrite, illite/smectite mixed layer, anatase, and calcite. Moreover, the bassanite had a high proportion in the floor rock.

The major-element oxides that were dominant were SiO_2, Al_2O_3, Fe_2O_3, and TiO_2, which is consistent with the kaolinite, pyrite, and anatase detected in the Shihao M8 coals. The trace elements in the coals were enriched in As and Cd and slightly enriched in Li, Cr, Co, Zr, Mo, Pb, and Tb. Other trace elements' content were significantly lower or close to the world's hard coals. The selected critical metals of Li, Sc, V, Ga, Nb, Zr, and REY, in the Shihao M8 coals did not reach the cut-off grades. However, the critical metals in the coal ashes were higher than in the world's hard coal ashes. The sediment source of the coals was predominantly the felsic–intermediate rocks atop the Kangdian Upland. The roof and floor samples were influenced by high-Ti basalt. The high degree of coalification of the coal samples from Songzao coalfields is related to the accumulation of mantle source materials from the Emeishan mantle plume. The parameters of sulfur content, coal ash component index, Sr/Ba, and Y/Ho reveal that the sedimentary environment of the Shihao coal suffered distinct seawater intrusion. Meanwhile, the Shihao coals were influenced by hydrothermal fluid during different coal-forming stages based on their mineralogical characteristics.

Author Contributions: Conceptualization, Methodology, Writing—original draft, Q.L.; Writing—review and editing, Funding acquisition, Supervision, S.Q.; Writing—review and editing, Funding acquisition, Supervision, W.W.; Formal analysis, Methodology, S.W.; Formal analysis, Methodology, F.S. All authors have read and agreed to the published version of the manuscript.

Funding: This research was funded by the National Natural Science Foundation of China (Nos. U1903207, 42172191, 41972176), the Science Foundation of Hebei (No. D2021402013), the Major Science and Technology Special Project of Xinjiang Uygur Autonomous Region (Nos. 2022A03014 and 2022A01002), and the Priority Academic Program Development of Jiangsu Higher Education Institutions (PAPD).

Data Availability Statement: All data of this study are available within the article.

Conflicts of Interest: The authors declare no conflict of interest.

References

1. BP P.L.C. *Bp Statistical Review of World Energy*, 71st ed.; BP P.L.C.: London, UK, 2022.
2. Dai, S.F.; Zhao, L.; Wei, Q.; Song, X.L.; Wang, W.F.; Liu, J.J.; Duan, P.P. Resources of critical metals in coal-bearing sequences in China: Enrichment types and distribution. *Chin. Sci. Bull.* **2020**, *65*, 3715–3729. (In Chinese with English Abstract) [CrossRef]
3. Dai, S.F.; Hower, J.C.; Finkelman, R.B.; Graham, I.T.; French, D.; Ward, C.R.; Eskenazy, G.; Wei, Q.; Zhao, L. Organic associations of non-mineral elements in coal: A review. *Int. J. Coal Geol.* **2020**, *218*, 103347. [CrossRef]
4. Jia, R.K.; Liu, J.J.; Han, Q.C.; Zhao, S.M.; Shang, N.D.; Tang, P.Q. Mineral matter transition in lignite during ashing process: A case study of Early Cretaceous lignite from the Hailar Basin, Inner Mongolia, China. *Fuel* **2022**, *328*, 125252. [CrossRef]
5. Hou, Y.J.; Dai, S.F.; Nechaev, V.P.; Finkelman, R.B.; Wang, H.D.; Zhang, S.W.; Di, S.B. Mineral matter in the Pennsylvanian coal from the Yangquan Mining District, northeastern Qinshui Basin, China: Enrichment of critical elements and a Se-Mo-Pb-Hg assemblage. *Int. J. Coal Geol.* **2023**, *266*, 104178. [CrossRef]
6. Ward, C.R. Analysis, origin and significance of mineral matter in coal: An updated review. *Int. J. Coal Geol.* **2016**, *165*, 1–27. [CrossRef]
7. Xu, F.; Qin, S.J.; Li, S.Y.; Wang, J.X.; Qi, D.E.; Lu, Q.F.; Xing, J.K. Distribution, occurrence mode, and extraction potential of critical elements in coal ashes of the Chongqing Power Plant. *J. Clean. Prod.* **2022**, *342*, 130910. [CrossRef]

8. Li, C.; Zhou, C.C.; Li, W.W.; Zhu, W.R.; Shi, J.Q.; Liu, G.J. Enrichment of critical elements from coal fly ash by the combination of physical separations. *Fuel* **2023**, *336*, 127156. [CrossRef]
9. Xiong, Y.; Ning, Z.P.; Liu, Y.Z.; Gomez, M.; Xiao, T.F. Emission and transformation behaviors of trace elements during combustion of Cd-rich coals from coal combustion related endemic fluorosis areas of Southwest, China. *Ecotoxicol. Environ. Saf.* **2022**, *246*, 114145. [CrossRef] [PubMed]
10. Duan, P.P.; Wang, W.F.; Liu, X.H.; Qian, F.C.; Sang, S.X.; Xu, S.C. Distribution of As, Hg and other trace elements in different size and density fractions of the Reshuihe high-sulfur coal, Yunnan Province, China. *Int. J. Coal Geol.* **2017**, *173*, 129–141. [CrossRef]
11. Dai, S.F.; Finkelman, R.B. Coal as a promising source of critical elements: Progress and future prospects. *Int. J. Coal Geol.* **2018**, *186*, 155–164. [CrossRef]
12. Dai, S.F.; Liu, C.Y.; Zhao, L.; Liu, J.J.; Wang, X.B.; Ren, D.Y. Strategic metal resources in coal-bearing strata: Significance and challenges. *J. China Coal Soc.* **2022**, *47*, 1743–1749. (In Chinese with English Abstract)
13. Dai, S.F.; Finkelman, R.B.; French, D.; Hower, J.C.; Graham, I.T.; Zhao, F.H. Modes of occurrence of elements in coal: A critical evaluation. *Earth-Sci. Rev.* **2021**, *222*, 103815. [CrossRef]
14. Qin, S.J.; Xu, F.; Cui, L.; Wang, J.X.; Li, S.Y.; Zhao, Z.S.; Xiao, L.; Guo, Y.X.; Zhao, C.L. Geochemistry characteristics and resource utilization of strategically critical trace elements from coal-related resources. *Coal Sci. Technol.* **2022**, *50*, 1–38. (In Chinese with English Abstract)
15. Chen, J.; Li, Y.; Jiang, P.J.; Zeng, J.; Chen, P.; Liu, W.Z.; Wang, X.M. Geochemistry of Neogene Mengtuo lignite in the Lincang from western Yunnan, southwestern China: Implications for its sediment material provenance and model of element enrichment. *Ore Geol. Rev.* **2021**, *139*, 104536. [CrossRef]
16. Qin, S.; Gao, K.; Sun, Y.; Wang, J.; Zhao, C.; Li, S.; Lu, Q. Geochemical Characteristics of Rare-Metal, Rare-Scattered, and Rare-Earth Elements and Minerals in the Late Permian Coals from the Moxinpo Mine, Chongqing, China. *Energy Fuels* **2018**, *32*, 3138–3151. [CrossRef]
17. Lu, Q.F.; Qin, S.J.; Wang, W.F.; Wang, Q.; Kang, S. Geochemistry of Late Permian coals from the Yueliangtian coal deposit, Guizhou: Evidence of sediment source and evaluation on critical elements. *Sci. Total Environ.* **2023**, *856*, 159123. [CrossRef] [PubMed]
18. Tang, Q.; Sheng, W.Q.; Li, L.Y.; Zheng, L.G.; Miao, C.H.; Sun, R.Y. Alteration behavior of mineral structure and hazardous elements during combustion of coal from a power plant at Huainan, Anhui, China. *Environ. Pollut.* **2018**, *239*, 768–776. [CrossRef] [PubMed]
19. Liu, J.J.; Dai, S.F.; Song, H.J.; Nechaev, V.P.; French, D.; Spiro, B.F.; Graham, I.T.; Hower, J.C.; Shao, L.Y.; Zhao, J.T. Geological factors controlling variations in the mineralogical and elemental compositions of Late Permian coals from the Zhijin-Nayong Coalfield, western Guizhou, China. *Int. J. Coal Geol.* **2021**, *247*, 103855. [CrossRef]
20. Lu, Q.F.; Qin, S.J.; Xu, F.; Chang, X.C.; Wang, W.F. Maceral and Organic Geochemical Characteristics of the Late Permian Coals from Yueliangtian Mine, Guizhou, Southwestern China. *ACS OMEGA* **2021**, *6*, 3149–3163. [CrossRef]
21. Li, B.Q.; Zhuang, X.G.; Li, J.; Querol, X.; Font, O.; Moreno, N. Geological controls on mineralogy and geochemistry of the Late Permian coals in the Liulong Mine of the Liuzhi Coalfield, Guizhou Province, Southwest China. *Int. J. Coal Geol.* **2016**, *154–155*, 1–15. [CrossRef]
22. Li, B.Q.; Zhuang, X.G.; Li, J.; Querol, X.; Font, O.; Moreno, N. Enrichment and distribution of elements in the Late Permian coals from the Zhina Coalfield, Guizhou Province, Southwest China. *Int. J. Coal Geol.* **2017**, *171*, 111–129. [CrossRef]
23. Zhuang, X.G.; Su, S.C.; Xiao, M.G.; Li, J.; Alstuey, A.; Querol, X. Mineralogy and geochemistry of the Late Permian coals in the Huayingshan coal-bearing area, Sichuan Province, China. *Int. J. Coal Geol.* **2012**, *94*, 271–282. [CrossRef]
24. Chen, J.; Chen, P.; Yao, D.X.; Liu, Z.; Wu, Y.S.; Liu, W.Z.; Hu, Y.B. Mineralogy and geochemistry of Late Permian coals from the Donglin Coal Mine in the Nantong coalfield in Chongqing, southwestern China. *Int. J. Coal Geol.* **2015**, *149*, 24–40. [CrossRef]
25. Dai, S.F.; Seredin, V.V.; Ward, C.R.; Hower, J.C.; Xing, Y.W.; Zhang, W.G.; Song, W.J.; Wang, P.P. Enrichment of U-Se-Mo-Re-V in coals preserved within marine carbonate successions: Geochemical and mineralogical data from the Late Permian Guiding Coalfield, Guizhou, China. *Miner. Depos.* **2015**, *50*, 159–186. [CrossRef]
26. Qin, S.J.; Gao, K.; Wang, J.X.; Li, Y.H.; Lu, Q.F. Geochemistry of the associated elements in the Late Permian coal from the Huoshaopu and Jinjia Mines, Southwestern Guizhou. *J. China Coal Soc.* **2016**, *41*, 1507–1516. (In Chinese with English Abstract)
27. Qin, S.; Lu, Q.; Gao, K.; Bo, P.; Wu, S. Geochemistry of elements associated with Late Permian coal in the Zhongliangshan mine, Chongqing, Southwest China. *Energy Explor. Exploit.* **2018**, *36*, 1655–1673. [CrossRef]
28. Li, B.Q.; Zhuang, X.G.; Querol, X.; Moreno, N.; Cordoba, P.; Shangguan, Y.; Yang, L.J.; Li, J.; Zhang, F. Geological controls on the distribution of REY-Zr (Hf)-Nb (Ta) enrichment horizons in late Permian coals from the Qiandongbei Coalfield, Guizhou Province, SW China. *Int. J. Coal Geol.* **2020**, *231*, 103604. [CrossRef]
29. Liu, J.J.; Nechaev, V.P.; Dai, S.F.; Song, H.J.; Nechaeva, E.V.; Jiang, Y.F.; Graham, I.T.; French, D.; Yang, P.; Hower, J.C. Evidence for multiple sources for inorganic components in the Tucheng coal deposit, western Guizhou, China and the lack of critical-elements. *Int. J. Coal Geol.* **2020**, *223*, 103468. [CrossRef]
30. Dai, S.F.; Wang, X.B.; Chen, W.M.; Li, D.H.; Chou, C.-L.; Zhou, Y.P.; Zhu, C.S.; Li, H.; Zhu, X.W.; Xing, Y.W.; et al. A high-pyrite semianthracite of Late Permian age in the Songzao Coalfield, southwestern China: Mineralogical and geochemical relations with underlying mafic tuffs. *Int. J. Coal Geol.* **2010**, *83*, 430–445. [CrossRef]

31. Zhao, L.; Ward, C.R.; French, D.; Graham, I.T. Mineralogical composition of Late Permian coal seams in the Songzao Coalfield, southwestern China. *Int. J. Coal Geol.* **2013**, *116–117*, 208–226. [CrossRef]
32. Zhao, L.; Ward, C.R.; French, D.; Graham, I.T. Major and Trace Element Geochemistry of Coals and Intra-Seam Claystones from the Songzao Coalfield, SW China. *Minerals* **2015**, *5*, 870–893. [CrossRef]
33. *GB/T 482-2008*; Sampling of Coal Seams. Chinese Management Committee of Standard Specifications: Beijing, China, 2008; p. 9.
34. *ASTM Standard D3173-11*; Standard Test Method for Moisture in the Analysis Sample of Coal and Coke. ASTM International: West Conshohocken, PA, USA, 2011.
35. *ASTM Standard D3174-11*; Standard Test Method for Ash in the Analysis Sample of Coal and Coke. ASTM International: West Conshohocken, PA, USA, 2011.
36. *ASTM Standard D3175-11*; Standard Test Method for Volatile Matter in the Analysis Sample of Coal and Coke. ASTM International: West Conshohocken, PA, USA, 2011.
37. *ASTM Standard D5865-13*; Standard Test Method for Gross Calorific Value of Coal and Coke. ASTM International: West Conshohocken, PA, USA, 2013.
38. *ASTM Standard D3177-02*; Standard Test Methods for Total Sulfur in the Analysis Sample of Coal and Coke. ASTM International: West Conshohocken, PA, USA, 2002.
39. *ASTM Standard D2492-02*; Standard Test Method for Forms of Sulfur in Coal. ASTM International: West Conshohocken, PA, USA, 2002.
40. *GB/T 16773-2008*; Method of Preparing Coal Samples for the Coal Petrographic Analysis. Chinese Management Committee of Standard Specifications: Beijing, China, 2008; p. 20.
41. Finkelman, R.B.; Dai, S.F.; French, D. The importance of minerals in coal as the hosts of chemical elements: A review. *Int. J. Coal Geol.* **2019**, *212*, 103251. [CrossRef]
42. Li, Y.; Huang, W.H.; Jiu, B.; Sun, Q.L.; Che, Q.S. Modes of Occurrence and Origin of Minerals in Permian Coals from the Huainan Coalfield, Anhui, China. *Minerals* **2020**, *10*, 399. [CrossRef]
43. Yan, X.Y. *Enrichment and Differentiation Mechanism of Minerals and Trace Elements in the Paleogene Coals from Baise area of Guangxi Province, China*; China University of Mining and Technology: Beijing, China, 2020; pp. 1–150.
44. Liu, J.J. *Occurrence Characteristics of Mineral Matters in Low-Rank Coals and Their Implications for Geological Process*; China University of Mining and Technology: Beijing, China, 2019; pp. 1–253.
45. Dai, S.F.; Zhou, Y.P.; Ren, D.Y.; Wang, X.B.; Li, D.; Zhao, L. Geochemistry and mineralogy of the Late Permian coals from the Songzao coalfield, Chongqing, southwestern China. *Sci. China Ser. D Earth Sci.* **2007**, *50*, 678–688. [CrossRef]
46. Knight, J.A.; Burger, K.; Bieg, G. The pyroclastic tonsteins of the Sabero Coalfield, north-western Spain, and their relationship to thestratigraphy and structural geology. *Int. J. Coal Geol.* **2000**, *44*, 187–226. [CrossRef]
47. Duan, P.P.; Wang, W.F.; Liu, X.H.; Sang, S.X.; Ma, M.Y.; Zhang, W. Differentiation of rare earth elements and yttrium in different size and density fractions of the Reshuihe coal, Yunnan Province, China. *Int. J. Coal Geol.* **2019**, *207*, 1–11. [CrossRef]
48. Chen, P.; Jiang, D.D. Characteristics and geological genesis of minerals in coals of Huainan. *J. Anhui Univ. Sci. Technol. Nat. Sci.* **2012**, *32*, 1–6. (In Chinese with English Abstract)
49. Dai, S.F.; Ren, D.Y.; Chou, C.L.; Finkelman, R.B.; Seredin, V.V.; Zhou, Y.P. Geochemistry of trace elements in Chinese coals: A review of abundances, genetic types, impacts on human health, and industrial utilization. *Int. J. Coal Geol.* **2012**, *94*, 3–21. [CrossRef]
50. Yan, X.Y.; Dai, S.F.; Graham, I.T.; He, X.; Shan, K.H.; Liu, X. Determination of Eu concentrations in coal, fly ash and sedimentary rocks using a cation exchange resin and inductively coupled plasma mass spectrometry (ICP-MS). *Int. J. Coal Geol.* **2018**, *191*, 152–156. [CrossRef]
51. Ketris, M.P.; Yudovich, Y.E. Estimations of Clarkes for carbonaceous biolithes: World average for trace element contents in black shales and coals. *Int. J. Coal Geol.* **2009**, *78*, 135–148. [CrossRef]
52. Taylor, S.R.; McLennan, S.H. *The Continental Crust: Its Composition and Evolution*; Blackwell: Oxford, UK, 1985; p. 312.
53. Dai, S.F.; Xie, P.P.; Jia, S.H.; Ward, C.R.; Hower, J.C.; Yan, X.Y.; French, D. Enrichment of U-Re-V-Cr-Se and rare earth elements in the late Permian coals of the Moxinpo Coalfield, Chongqing, China: Genetic implications from geochemical and mineralogical data. *Ore Geol. Rev.* **2017**, *80*, 1–17. [CrossRef]
54. Lu, Q.F.; Qin, S.J.; Bai, H.Y.; Wang, W.F.; Qi, D.E.; He, X.; Zhang, B.F. Geochemistry of rare earth elements and yttrium in Late Permian coals from the Zhongliangshan coalfield, Southwestern China. *Front. Earth Sci.* **2023**, *17*, 230–250. [CrossRef]
55. Dai, S.F.; Graham, I.T.; Ward, C.R. A review of anomalous rare earth elements and yttrium in coal. *Int. J. Coal Geol.* **2016**, *159*, 82–95. [CrossRef]
56. Shao, H.; Xu, Y.; He, B.; Huang, X.; Luo, Z. Petrology and geochemistry of the late stage acidic volcanic rocks of the Emeishan large igneous province. *Bull. Mineral. Petrol. Geochem.* **2007**, *26*, 350–358. (In Chinese with English Abstract)
57. Liu, J.J.; Han, Q.C.; Zhao, S.M.; Jia, R.K. The sources of abnormally enriched critical metals in the Late Permiancoals of Western Guizhou Province. *J. China Coal Soc.* **2022**, *47*, 1782–1794.
58. Chen, Z.S.; Wu, Y.D. Late Permian Emeishan Basalt and Coal-bearing Formation in Southern Sichuan Area. *Coal Geol. China* **2010**, *22*, 14–18.

59. Xiao, L.; Xu, Y.G.; Mei, H.J.; Zheng, Y.F.; He, B.; Pirajno, F. Distinct mantle sourcesof low-Ti and high-Ti basalts from the western Emeishan large igneous province, SW China: Implications for plume–lithosphere interaction. Earth and Planetary Science. *Letters* **2004**, *228*, 525–546. [CrossRef]
60. Chou, C.-L. Sulfur in coals: A review of geochemistry and origins. *Int. J. Coal Geol.* **2012**, *100*, 1–13. [CrossRef]
61. Zhao, S.Q. *Practical Coal Petrology*; Geological Publishing House: Beijing, China, 1991; p. 205.
62. Ye, D.M.; Luo, J.W.; Xiao, W.Z. *Maceral Properties and Its Application of Petrography in Southwest China*; Geological Publishing House: Beijing, China, 1997; p. 125.
63. Dai, S.; Bechtel, A.; Eble, C.F.; Flores, R.M.; French, D.; Graham, I.T.; Hood, M.M.; Hower, J.C.; Korasidis, V.A.; Moore, T.A.; et al. Recognition of peat depositional environments in coal. A review. *Int. J. Coal Geol.* **2020**, *219*, 103383. [CrossRef]
64. Xie, P.P.; Song, H.J.; Wei, J.P.; Li, Q.Q. Mineralogical Characteristics of Late Permian Coals from the Yueliangtian Coal Mine, Guizhou, Southwestern China. *Minerals* **2016**, *6*, 29. [CrossRef]
65. Wang, P.P. *Enrichment and Differentiation Mechanism of Minerals and Trace Elements in the Late Permian Coals from Eastern Yunnan and Western Guizhou Province*; China University of Mining and Technology: Beijing, China, 2017; pp. 1–179.
66. Han, D.X. *Coal Petrology of China*; China University of Mining and Technology Press: Xuzhou, China, 1996. (In Chinese)
67. Zhao, L.X. *Enrichment Mechanism of Rare Metals in Coal-Hosted Niobium Predominated Polymetallic Ore Deposit from the Late Permian Strata, Northeastern Yunnan Province, Southwest China*; China University of Mining and Technology: Beijing, China, 2016.
68. Ward, C.R. Analysis and significance of mineral matter in coal seams. *Int. J. Coal Geol.* **2002**, *50*, 135–168. [CrossRef]
69. Seredin, V.V.; Dai, S.F. Coal deposits as potential alternative sources for lanthanides and yttrium. *Int. J. Coal Geol.* **2012**, *94*, 67–93. [CrossRef]